1-1-2016

Cell compatible encapsulation of filaments into 3D hydrogels

Katharina Schirmer
University of Wollongong, ksus852@uowmail.edu.au

Robert A. Gorkin III
University of Wollongong, rgorkin@uow.edu.au

Stephen T. Beirne
University of Wollongong, sbeirne@uow.edu.au

Elise M. Stewart
University of Wollongong, elises@uow.edu.au

Brianna C. Thompson
University of Wollongong, brianna@uow.edu.au

See next page for additional authors

Cell compatible encapsulation of filaments into 3D hydrogels

Abstract

Tissue engineering scaffolds for nerve regeneration, or artificial nerve conduits, are particularly challenging due to the high level of complexity the structure of the nerve presents. The list of requirements for artificial nerve conduits is long and includes the ability to physically guide nerve growth using physical and chemical cues as well as electrical stimulation. Combining these characteristics into a conduit, while maintaining biocompatibility and biodegradability, has not been satisfactorily achieved by currently employed fabrication techniques. Here we present a method combining pultrusion and wet-spinning techniques facilitating incorporation of pre-formed filaments into ionically crosslinkable hydrogels. This new biofabrication technique allows the incorporation of conducting or drug-laden filaments, controlled guidance channels and living cells into hydrogels, creating new improved conduit designs.

Disciplines

Engineering | Physical Sciences and Mathematics

Publication Details

Authors

Katharina Schirmer, Robert A. Gorkin III, Stephen T. Beirne, Elise M. Stewart, Brianna C. Thompson, Anita F. Quigley, Robert M. I Kapsa, and Gordon G. Wallace

Cell Compatible Encapsulation of Filaments into 3D Hydrogels

Katharina S.U. Schirmer[1], Robert Gorkin III[1], Stephen Beirne[1], Elise Stewart[1], Brianna C. Thompson[1], Anita F. Quigley[1,2], Robert M.I. Kapsa[1,2] and Gordon G. Wallace[1]

[1] ARC Centre for Electromaterials Science, Intelligent Polymer Research Institute, University of Wollongong, Wollongong NSW, Australia
[2] Department of Clinical Neurosciences, St Vincent's Hospital, Melbourne and Department of Medicine, The University of Melbourne, VIC, Australia

1.1 Abstract

Tissue engineering scaffolds for nerve regeneration, or artificial nerve conduits, are particularly challenging due to the high level of complexity the structure of the nerve presents. The list of requirements for artificial nerve conduits is long and includes the ability to physically guide nerve growth using physical and chemical cues as well as electrical stimulation. Combining these characteristics into a conduit, while maintaining biocompatibility and biodegradability, has not been satisfactorily achieved by currently employed fabrication techniques. Here we present a method combining pultrusion and wet-spinning techniques facilitating incorporation of pre-formed filaments into ionically crosslinkable hydrogels. This new biofabrication technique allows the incorporation of conducting or drug-laden filaments, controlled guidance channels and living cells into hydrogels, creating new improved conduit designs.

1.2 Introduction

Manufacturing complex scaffolds which truly mimic natural tissue is one of the greatest ongoing challenges for biofabrication [1]. Critically, these structures must match the intrinsic geometry and functionality of the body's environment to develop treatments for conditions where artificial tissues or structures are essential [1, 2]. Engineering scaffolds for regenerative peripheral nerve applications is particularly difficult as many biological, physical, and chemical requirements need to be fulfilled [3]. This challenge has been outlined in a number of reviews which detail required characteristics to build an *ideal* conduit and facilitate nerve regeneration [4-6]. The *ideal* conduit that has been proposed needs to be biocompatible, biodegradable, and have appropriate porosity to allow exchange of fluids, gasses and nutrients, while preventing unwanted cells from penetrating into the structure [7]. Strategies for these conduits also include controlled drug and growth factor release to provide

1

chemical cues to the regenerating nerve contributing to the ideal environment for regrowth [8]. Integrating conductivity within the conduit has additionally been suggested as a way to facilitate electrical stimulation of nerve cells, which has been shown to have positive effects on the regeneration process [9]. Further, to structurally mimic the nerve and provide guidance to the regenerating cells small channels or lumens need to be incorporated into the design [10]. Finally, inclusion of supportive cells like Schwann cells can further provide guidance and chemical stimulation by releasing growth factors and hence improve the regeneration of the nerve [8].

Efforts to address these requirements have often focused on developing material systems to meet one or two characteristics of the ideal conduit at a time and assembling them into a final structure. For instance, by electrospinning drug-loaded silk mats and manually rolling them into a tube, Dinis *et al*. [11] fabricated a slow release, multi-luminal, but non-degradable nerve conduit that closely mimicked the mechanical properties and morphological structure of nerves. Abidian *et al*. [12] manufactured a partially-degradable, conducting, single lumen 3D hydrogel conduit in a multi-step approach utilizing sputter coating, dip coating and electro-polymerization, as well as chemical treatments to dissolve parts of the construct, creating the inner lumen. A conducting pattern was created by manually covering parts of the structure with masking tape before electrically polymerizing a conducting polymer onto the surface. Lee *et al*. [13] implanted a non-degradable, porous, collagen coated electrode-conduit system into a rat model and delivered electrical stimulation to the regenerating nerve. Using a multi-step approach our group has previously fabricated a conduit combining biodegradability, precise pore sizes, internal guidance and (uncontrolled) growth factor delivery (Quigley *et al*. [14]). This conduit was produced using sequential fabrication and assembly processes, including wet spinning, electrospinning, knitting and drop-casting of multiple components before manual assembly.

The fabrication of the examples above required multiple production steps and manufacturing technologies and significant manual assembly. So far the design and manufacture of a universal platform able to integrate the ideal features into a single structure has been limited by currently employed fabrication techniques. A less complicated approach would be desirable to increase quality and repeatability in production of the conduits and reduce the complexity and costs of fabrication without compromising on the conduits performance.

2

Reduced to their most basic morphological features, nerves and nerve guides or conduits are tubular structures and several leading fabrication approaches have been used to create scaffolds that conform to this general form [15-17]. Wet-spinning is a well-established, versatile fabrication technique that has been used to produce long homogenous bio-fibres with diameters ranging from nanometres to millimetres [18-21]. During wet-spinning, the spinning solution is passed through a nozzle or spinneret and into a bath that contains the material's specific coagulation agent. Fibres either remain in the bath to coagulate, or more commonly are gathered on a collector drum after coagulation. The drum can also be used to draw the fibres during the spinning process, resulting in smaller fibre diameters and increased mechanical properties in some materials [22]. The cross-sectional shape and size of the fibre are mainly dictated by dimensions of the extrusion nozzle, the extrusion rates used and the post-spinning treatment applied to the fibre.

Commonly used materials for wet spinning bio-fibres are ionically crosslinkable hydrogels like sodium alginate or gellan gum. These materials can easily be wet-spun into fibres using calcium containing coagulation baths. Fibres produced in this way show biocompatibility with a range of cell types which are in contact with or encapsulated into the fibres. Alginate in particular, has been used frequently to produce viable-cell laden fibres due in part to the mild conditions under which fibres can be produced (aqueous systems, neutral pH, no harsh solvents or high temperatures)[23, 24]. However, these hydrogels alone cannot achieve all the features needed for an ideal nerve guide, as they lack inherent controllable drug or growth factor release as well as the presence of electrical conductivity in the bulk material for stimulation. As such, alginates are often combined with other materials such as polylactic acid and organic electrically conducting materials like conducting polymers or graphenes, which show excellent drug delivery profiles and electrical conductivity [25-29]. These secondary components are easily produced in different shapes, including films, particles and fibres.

In order to address the lack of inherent electrical conductivity and ability to deliver drugs in a controlled fashion, a novel technique has been developed, which combines the processability of ionically crosslinked hydrogels with the desired properties of secondary material components by controllably embedding pre–formed filaments into hydrogels. This method allows not only the encapsulation of reliably conducting or drug releasing elements, but also enables encapsulation of living cells into the 3D system. Here we present the design, testing and optimization of the system and also showcase its flexibility by producing fibrous 3D

3

hydrogels containing filaments of different materials, morphologies and geometries, placed controllably into a range of positions and configurations. Furthermore, we investigate the production of homogenous channels in the hydrogels by mechanically removing the encapsulated filaments as well as backfilling these channels with other liquids. The cytocompatibility of the fabrication method and the resulting 3D structures were also investigated by extruding living cells directly into the 3D structure and analysing their viability at different time points after production.

1.3 Experimental

1.3.1 Materials

Medium viscosity alginate (Alg_M, Sigma-Aldrich, Australia) and ultrapure, low viscosity alginate (Alg_L, Pronova, USA) were used to encapsulate filaments into fibrous 3D structures. Alginate stock solutions were prepared by dissolving the respective alginate powder in water at 20 mg ml^{-1}. Stock solutions were kept at 4°C and used within 8 weeks of preparation. Spinning solutions containing less than 20 mg ml^{-1} alginate were prepared by diluting from stock solutions. 90 mM calcium chloride ($CaCl_2$, ChemSupply, Australia) was used as the coagulation solution for all experiments.

The filaments used are summarized in Table 1 and filament specific dimensions, shapes, properties (roughness, hydrophobicity) and manufacturers are detailed. To assist the reader abbreviations for the filaments referenced throughout the article are also outlined.

Table 1: Summary of abbreviations, materials, diameters and manufacturers of filaments used as part of this study.

Abb.	Material	Diameter	Properties	Manufacturer
SS_{50}	316 stainless steel	50 μm	circular, very smooth, hydrophilic	Goodfellow, UK
SS_{150}	316 stainless steel	150 μm	circular, very smooth, hydrophilic	Goodfellow, UK
Fe_{65}	Iron	65 μm	circular, smooth, hydrophilic	Goodfellow, UK
PLA_{100}	polylactic acid	115 μm	mostly circular, smooth, hydrophilic	made in-house
PLA_+	polylactic acid	100 μm	star shaped, smooth, hydrophobic	made in-house
rGO-PPy	80% graphene 20% polypyrrole	150 μm	mostly circular, rough, very hydrophobic	made in-house
CFT	carbon fibre tow	-	bundle, rough, hydrophobic	SGL group, Germany
Nylon	nylon fishing line	280 μm	circular, very smooth, very hydrophobic	Jarvis Walker, Australia

Commercially available filaments were used as received, with exception of CFT which was manually pulled into small bundles containing 20 – 50 fibres. PLA and rGO-PPy composite fibres were produced in-house using either melt or wet-spinning methods respectively. PLA fibres were produced by means of a counter rotating micro twin-screw extruder (Burrell

Scientific, USA). The extruded filaments were drawn at ambient temperature to a diameter of 100 - 150 µm and collected on a winder.

rGO-PPy composite fibres were produced by using a rotational wet-spinning approach as described in Schirmer *et al.* [30]. The spinning solutions were prepared by adding PPy nanoparticles to graphene oxide dispersed in water at a weight ratio of 80% graphene and 20% PPy particles. Fibres were extruded through a 19 gauge single lumen metal spinneret at a rate of 25 ml h^{-1}. A coagulation bath was used to form the fibres which contained a mixture of ethanol, acidic reducing agent and calcium chloride. Fibres remained in the coagulation bath at 80°C for 12 h; then were washed, collected and dried in air.

1.3.2 Fabrication Method

The setup for the customized wet-spinning based pultrusion method is illustrated in Figure 1A. Purpose-built, custom spinnerets with continuous through-channels to feed and encapsulate filaments are core to the method. A transverse section of an example of a spinneret accommodating four filaments is shown in Figure 1B. Filaments are passed straight through the spinnerets, while a hydrogel is fed into the main barrel through a separate port, resulting in the encapsulation of the filaments. A dual syringe pump (Gemini 88, KD Scientific) was installed vertically to extrude the spinning solutions at precisely controlled rates through the spinneret into the coagulation bath. To allow formation of the 3D structure, the coagulation bath was secured on a motorised linear stage to move the bath in a fixed plane relative to the spinneret at variable controllable speeds. Operation of the 24 V linear stage (Cool Muscle RCM1) was managed through proprietary control software (Cool Works Lite 4.1.4) that provides an interface to define parameters including, position, acceleration, and velocity.

Before the extrusion process was initiated, filaments were threaded through the spinneret, aligned, and secured within the coagulation bath using custom 3D printed titanium holders. The spinneret was then connected to the syringe containing the hydrogel solution and placed in the first position in the syringe pump. If an additional spinning solution was required, it was placed into the second position in the syringe pump and connected to the spinneret via a piece of tubing, as shown in Figure 1A and Figure 1D respectively.

Once these steps were completed the filament was put under tension and the coagulation solution was filled into the bath until the horizontal barrel of the spinneret was fully submerged.
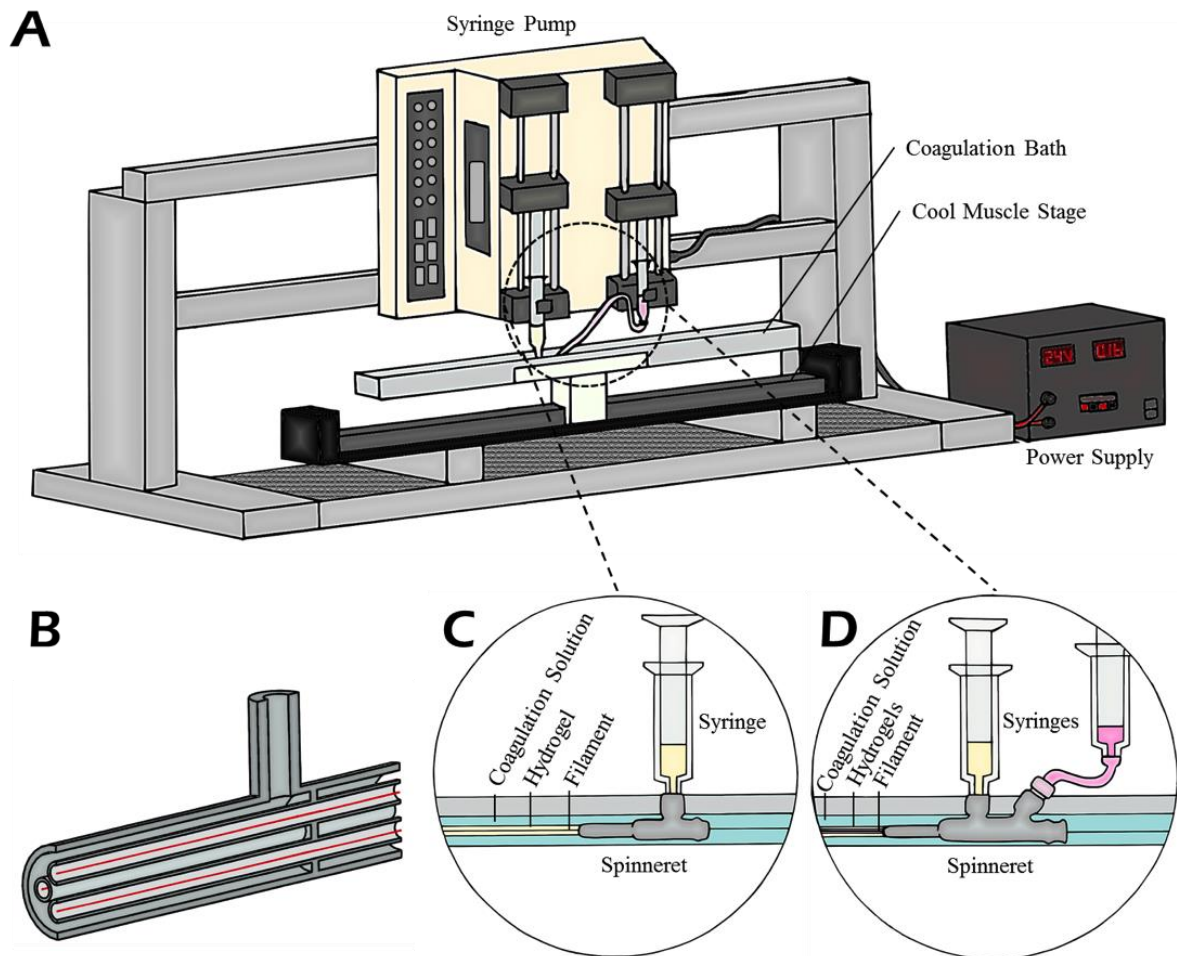
Figure 1: Schematic setup of filament encapsulating extrusion system (A). B: Exemplary transverse section of spinneret. Insets show the pultrusion process is illustrated in Figure 2. The procedure is initiated by starting the syringe pump and pumping the hydrogel solution from the syringe through the spinneret and into the coagulation bath (Figure 2A1-3). Once the hydrogel is observed to exit the spinneret, the stage is set into motion, starting with the end of the coagulation bath close to the front tip of the spinneret and moving to the opposite side. As the coagulation bath is moved away from the spinneret, the gel was continually extruded, surrounding the installed filament/s, forming a structure which encapsulates the filament/s (Figure 2B1-2). The extrusion and stage movement continue until the back end of the spinneret has reached the end of the coagulation bath, or when the desired length of extrusion has been reached. The extruded structure was then removed from the set-up by severing at the attached end and in front of the spinneret (Figure 2C1-3).

The pultrusion process is illustrated in Figure 2. The procedure is initiated by starting the syringe pump and extruding the hydrogel solution from the syringe through the spinneret and into the coagulation bath (Figure 2A1-A3). Once the hydrogel exits the spinneret, the stage is set into motion, moving the coagulation bath, which in turn moves the spinneret horizontally through the coagulation solution from one end of the bath to the other, at a controlled rate. As the coagulation bath is moved, the gel is continually extruded, surrounding and encapsulating the installed filament/s (Figure 2B1-B2). The extrusion and stage movement continue until the back end of the spinneret has reached the end of the coagulation bath, or when the desired length of extrusion has been achieved. The extruded structure is then removed from the set-up by severing the end attached to the spinneret (Figure 2C1-C3).
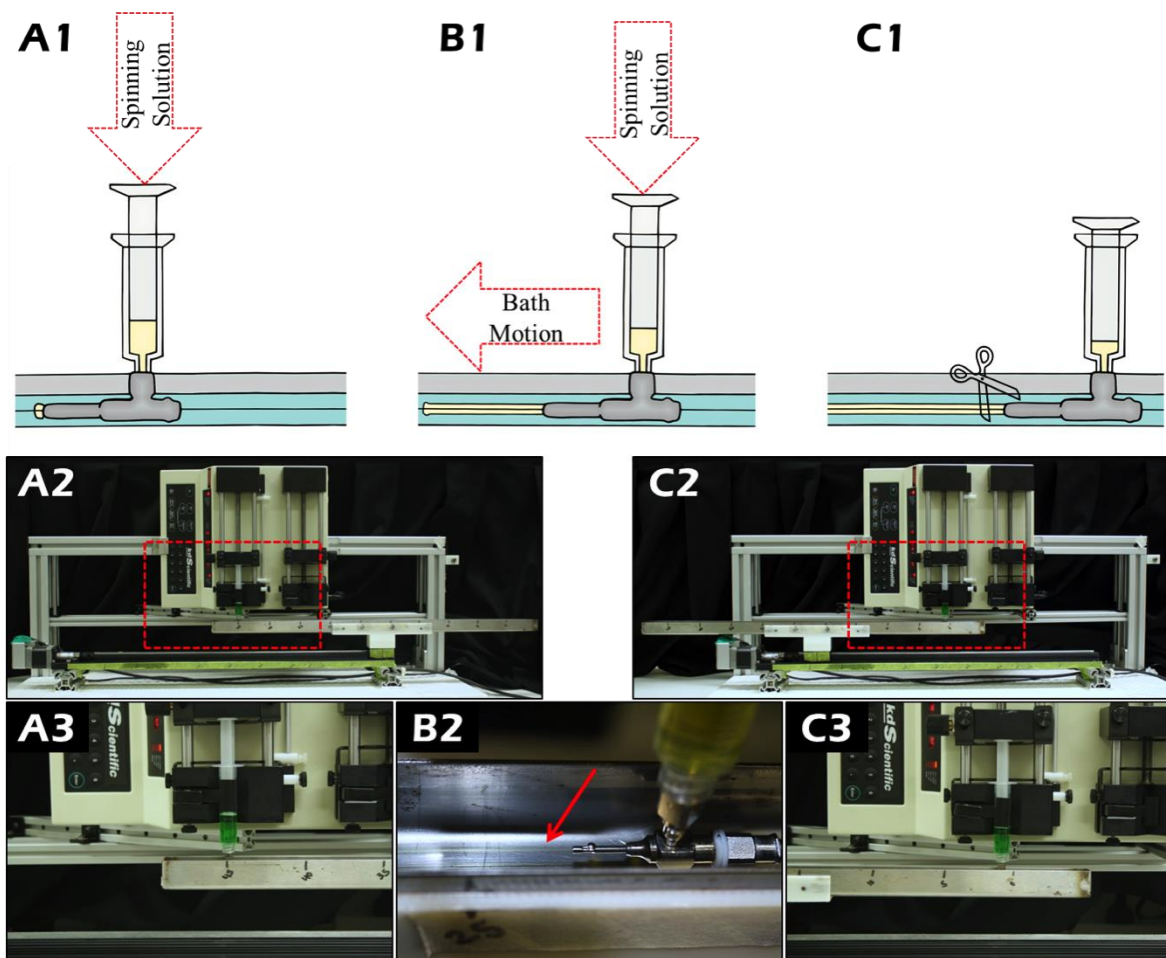
Figure 2: Illustration of the extrusion process. A: The spinning solution is pushed through the spinneret and into the coagulation bath. B: While the extrusion of the spinning solution continues, the bath starts moving away from the spinneret, resulting in the hydrogel to be extruded around the filament. C: When the extrusion is completed, both stage and syringe pump are stopped and the extruded structure removed from the bath.

A critical part of the assembly is the exact positioning of the filaments, which need to be reliably aligned with the spinneret and held under tension throughout the pultrusion process to ensure even encapsulation. This was achieved by designing a custom filament holder as shown in Figure 3: an array of fine holes (Ø 400 μm) allow filament positioning in different configurations to enable the use of the holder with a range of commercial and custom spinnerets. Larger holes were incorporated into the design to allow unimpeded fluid flow through the holder and prevent any baffling effect during the extrusion process. The holder rests on the side wall of the coagulation bath anywhere along its length and is secured in place by M4 screws. The filament holders were 3D printed (titanium 6-4, powder of spherical particles 20-60 μm distribution in 25 μm layers) using a SLM-50 metal additive fabrication system (Realizer, Germany). Post-treatment of the printed parts to achieve a smoothened

surface finish involved the removal of support material, bead blasting (20 μm glass beads) and bath sonication in water to remove loose material.
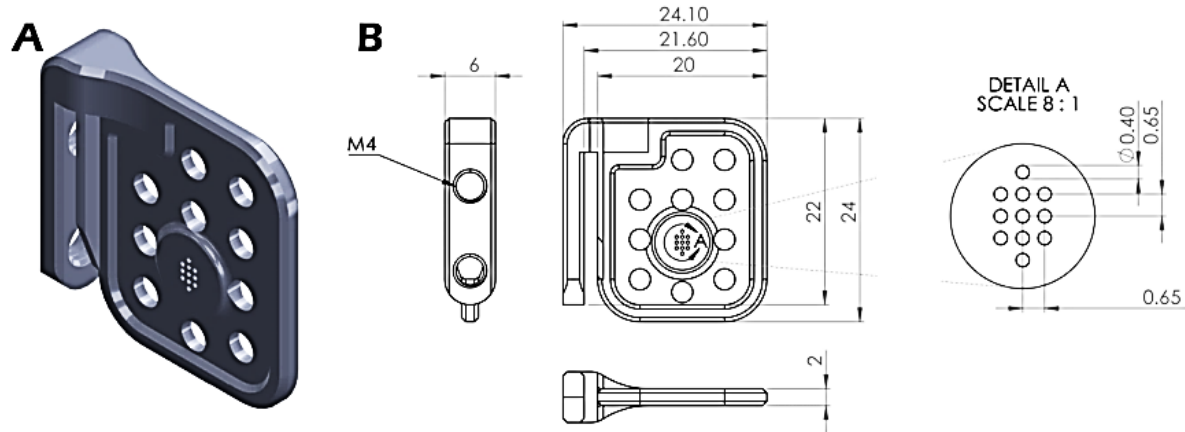
Figure 3: Rendered view (A) and technical drawing (B) of filament holder including enlarged detail view of positioning of holes which hold the filaments in place. All measurements are in mm.

The coagulation bath was folded and welded from stainless steel sheets to a length of 750 mm, with a width and depth of 25 mm. The length of the bath was chosen to use the entire moving range of the linear stage in order to maximize the length of filament that could be encapsulated in one extrusion event (65 cm). The width and depth were kept to a minimum to reduce the amount of coagulant required to fill the bath, in order to reduce the weight that has to be moved.

1.3.3 Controllability, Reproducibility and Versatility

Controllability and reproducibility of the system were analysed by the production of fibres from Alg_M extruded around Fe_{65} at different combinations of extrusion rates and stage speeds. The resulting fibre diameters extruded under the same conditions were compared within batches as a measure of reproducibility and between fabrication runs to assess the instruments limitations and flexibility with respect to the hardware.

To analyse the response of the system to changing stage speeds and extrusion rates different thickness gradients were produced. Gradual diameter gradients along the gel structure were produced by extrusion around Fe_{65} while manually varying the extrusion rates between $0.1 - 0.8$ ml min^{-1} with a constant stage speed (4.8 mm sec^{-1}). Abrupt changes in diameter were produced by varying the stage speeds during the extrusion process between $3.6 - 24.1$ mm sec^{-1}, while keeping the extrusion rate constant 0.3 ml min^{-1}.

8

To investigate the versatility of the method, a variety of spinneret designs were utilized to fabricate structures with different filament layouts using a range of filament sizes (50 – 290 µm diameter), shapes and materials.

1.3.4 Incorporation of Living Cells

To incorporate cells into the conduits, the setup was sterilized and moved into a Class II biosafety cabinet. Instrumentation not suitable for autoclaving (syringe pump, power supply, stage, tubing) was sterilized using 70% ethanol. All other parts (coagulation bath, spinneret, holders, SS wires) were autoclaved at 121°C for 20 minutes. 90 mM calcium chloride coagulation solution and Alg_L spinning solution diluted to 1% were filter sterilized using 0.2 µm sterile cellulose filters (Merck Millipore, Australia).

The extrusion process was performed at room temperature. To decrease the period of time cells were exposed to ambient temperatures and maintain high viability, cells were suspended in gels warmed to 37°C shortly before pultrusion and transferred into media warmed to 37°C immediately after finishing the extrusion process.

A neuronal PC12 cell line used in the work, was cultured by splitting routinely every two to three days when semi-confluent using 0.05% Trypsin (Life Technologies, Australia) following the protocols from the American Type Culture Collection (ATCC). Cells were maintained in proliferation medium containing Dulbecco's Modified Eagle's Medium (DMEM, Invitrogen, Australia), 10% horse serum (Sigma), 5% fetal bovine serum (FBS, Bovogen) and 2 mM Glutamine (Life Technologies).

For incorporation in the extrusion process, PC12 cells were counted and resuspended in 1% Alg_L at a density of 5×10^5 cells ml^{-1}. Cell-laden gel was pipetted up and down several times to ensure that the cells were well dispersed within the gel, before it was being transferred into a sterile syringe.

For viability studies cell-laden fibres were extruded using a four lumen spinneret and four SS_{50} filaments with the stage speed set to 4.8 mm sec^{-1} and an extrusion rate of 0.5 ml min^{-1}. Cells in fibres were stained for live and dead cells (described in Section 1.3.5) at 3 h, 24 h and 4 days after extrusion.

For fabrication of 3D gel fibres containing cells in a middle lumen and four SS_{50} filaments, cells were suspended in a gellan gum microgel, which was prepared based on a modified bio-ink protocol [31]. Briefly, 0.5 ml of 1% filter sterilized gellan gum (Gelzan CM, Sigma-

Aldrich) solution and 9.5 ml DMEM were heated separately to 80°C before being mixed together in a 50 ml centrifugation tube and vortexed until cooled to room temperature. The resulting gellan gum microspheres keep cells homogenously suspended in solution, which overcomes cell settling issues during the extrusion process. Cells were suspended in gellan gum microgel at a density of 1.5×10^6 cells ml^{-1} and extruded through the innermost needle at a rate of 0.05 ml min^{-1}. A 1% Alg$_L$ solution was fed into the outer needle of the spinneret at a rate of 0.8 ml min^{-1}, with the stage speed set to 4.8 mm sec^{-1}.

For fabrication of triaxial fibres, cells dispersed in 2% Alg$_L$ were extruded in the middle lumen around one filament of SS$_{50}$ at a rate of 0.05 ml min^{-1}, while 2% Alg$_L$ without cells was extruded through the outer needle at a rate of 0.4 ml min^{-1}. The stage speed was set to 4.8 mm sec^{-1}.

1.3.5 Cell Staining and Imaging

Calcein acetoxymethyl ester (Calcein AM, Life Technologies, stock concentration: 1 mg ml^{-1}) and propidium iodide (PI, Life Technologies, stock concentration: 1 mg ml^{-1}) were used to fluorescently label live and dead cells respectively. Staining solutions were prepared separately by diluting Calcein AM 1:500 and PI 1:1000 in DPBS (Dulbecco's phosphate buffered saline, Life Technologies). Cells were incubated with Calcein AM staining solution for 15 minutes at 37°C, followed by addition of PI staining solution and 5 minutes further incubation at room temperature, before the Leica TSC SP5 II confocal microscope and LAS AF version 2.6.3.8173 software were used to obtain z-slices and stacks of fluorescently labelled cells cultured in 3D gels. Numbers of live and dead cells in each z-slice image were counted using the cell counting plugin of ImageJ software. A minimum of 10 images per time point, taken at different positions of the 3D structure were analysed. One way ANOVA was used to determine significant differences between cell numbers at a confidence level of 0.05.

1.3.6 Imaging and Microscopy

Brightfield microscope images were taken using a Leica DM IL LED (Germany) with LAS software version 4.0. A confocal microscope (Leica TSC SP5 II) was used to image cells and obtain digital micrographs. Scanning electron microscopy images of gel cross-sections were obtained after freezing and sectioning the samples in liquid nitrogen. Imaging was performed using a low-vacuum JEOL JSM 6490LV.

1.4 Results and Discussion

1.4.1 Controllability, Reproducibility and Flexibility

To evaluate the controllability and reproducibility of gel fibre diameters resulting from the extrusion process, Alg_M was extruded around a single Fe_{65} filament using the coaxial spinneret. The extrusion rate was set to 0.3, 0.5 or 0.7 ml min^{-1} respectively with stage speeds varying between 2.4 – 21.6 mm sec^{-1}. Four stage speeds were used per extrusion event over the length of 65 cm, with each speed held for a distance of around 15 cm. To distinguish between stage speeds a small low speed phase (stage speed 1.2 mm sec^{-1} over 1 cm) was introduced between each speed section (Figure 4A).

The order in which stage speeds were used along the length of each extrusion event was selected randomly to eliminate the potential influence of previous speeds on the resulting gel diameter. All combinations of stage speeds and extrusion rates were repeated three times in varying combinations of speeds per extrusion event. Once the extrusion was completed, the extruded gel was separated into one piece per speed section that was cut into five pieces each. Images were taken using the Leica M205A microscope with LAS 4.0 software. On each section, the diameter was measured in three locations (towards each end and in the middle) using ImageJ. The data of all sections produced using the same parameters were pooled together and analysed.

As expected, the fibre diameter decreases with a reduction in extrusion rate and an increase in stage speed, as shown in Figure 4D. The diameters of gels extruded at the same extrusion rates follow a power function. At lower stage speeds an increase therefore results in a significant reduction of the extruded gel diameter. At higher stage speeds, an increase of the speed still results in a reduction of fibre diameter, albeit a much smaller one.

As can be seen from the small errors, the variation in gel diameter was minimal, averaging $3 \pm 0.9\%$ of the measured diameter. For fibres extruded at a rate of 0.3 ml min^{-1} the deviation of diameters was the largest, averaging $3.8 \pm 0.7\%$, while diameters of gels extruded at 0.5 ml min^{-1} and 0.7 ml min^{-1} showed a deviation of $2.6 \pm 0.9\%$ and $2.9 \pm 0.5\%$ respectively. The difference in consistency of the fibres could be a result of better or poorer match of extrusion rates for the spinneret. If the extrusion rates are well matched to the flow area of the spinneret, the gel can form evenly around the fibre, without causing disruptions or disturbance at the exit of the spinneret, resulting in a more homogenous gel encapsulated fibre. Images B – D in Figure 4 show examples of the fibre diameters that can be achieved

11

with the same spinneret, by varying the extrusion rate and stage speed. Without sacrificing precision and uniformity, a wide range of desired gel diameters can be produced.
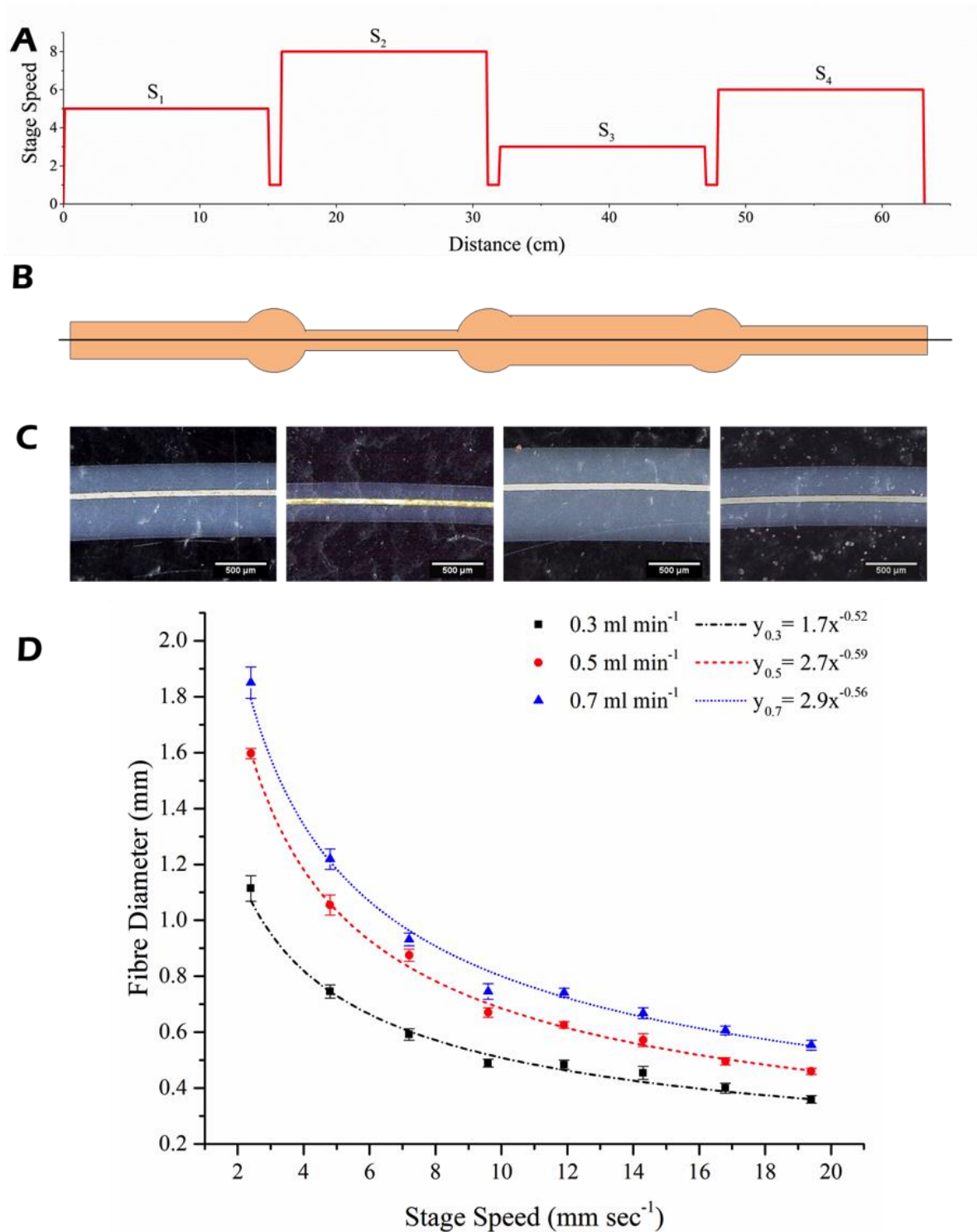

Figure 4: Speed over distance diagram illustrating the method (A) used to produce fibres of different diameters within one extrusion event, using four different speeds ($S_1 - S_4$ (A)) while applying a constant gel extrusion rate. The short low speed sections between the constant speeds are implemented to distinguish between the applied speeds in the finished extrusion as illustrated in B. C: Representative images of the resulting gel sections produced in one extrusion event. Gel encapsulated fibre diameter as a function of the stage speed (D) at three extrusion rates (0.3, 05 or 0.7 ml min^{-1}).

By keeping either the extrusion rate or the stage speed constant and varying the other, gel structures with thickness gradients like those shown in Figure 5 can be created. Keeping the stage speed constant and applying a variety of extrusion rates throughout the extrusion event will lead to the formation of gentle gradients in the overall diameter of the gel fibre. To create more abrupt changes in diameter the extrusion rate is kept constant, while the stage speed is varied. As shown in Figure 5B the average distance over which the diameter change can be created is around 3 mm with an extrusion rate of 0.3 ml min^{-1}. Over this distance the fibre diameter can be halved or doubled by applying stage speeds with a difference of 15 – 18 mm sec^{-1}. The distance over which the fibre diameter changes can be tailored by changing the extrusion rate (lower rates will lead to a shorter distance). The difference in fibre diameter is controlled by the difference between the stage speed settings (larger differences will lead to a larger change in diameter).
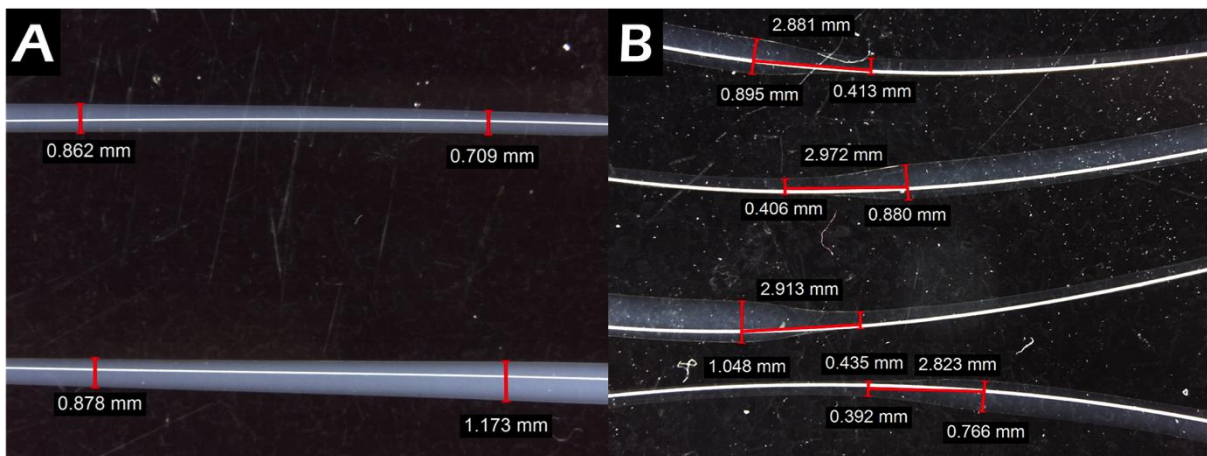
Figure 5: Thickness gradients of gel around a 50 µm stainless steel wire resulting from A: varying extrusion rates (0.3 – 0.7 ml min^{-1}, distance between measurements 11 mm) used throughout the extrusion process with a constant stage speed (speed 4.8 mm sec^{-1}) and B: through a constant extrusion rate (0.3 ml min^{-1}) and varying stage speeds (2.4 – 21.6 mm sec^{-1}).

By using one spinneret and one type of filament, a large variety of fibrous 3D structures can be produced in a very controlled fashion. Gel diameters from 0.4 - 2 mm can be fabricated readily, in single or multiple extrusion events, creating consistent and gradually or rapidly increasing or decreasing sizes.
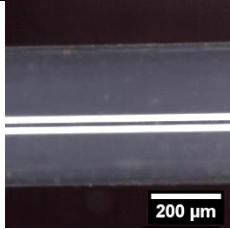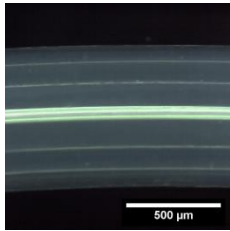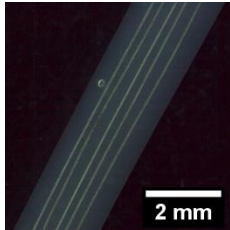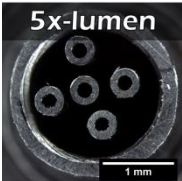
1.4.2 Versatility

To further expand and explore the versatility of the system a range of spinnerets were studied. All spinnerets were custom fabricated (Rame Hart Instrument, USA). Fibre images in Table 2 show that high complexity of the hydrogel structures can be achieved by changing the spinneret design, allowin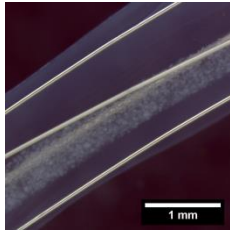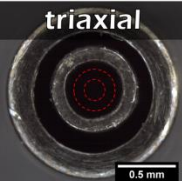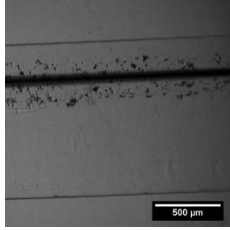g for positioning of filaments virtually anywhere within the gel. The number of encapsulated filaments can be varied, however limitations apply eventually, as the spacing between the needles carrying filament needs to be sufficient to allow unimpeded flow of gel around each filament. If gels of lower viscosity are used this spacing can be smaller, compared to applications where a high viscosity spinning solution is required. The ideal design needs to be evaluated on an individual basis taking into consideration the range of viscosities of spinning solutions, desired overall diameter of the structure as well as coagulation speed of the spinning solution.

Table 2 summarises each spinneret's dimensions and resulting gel structure layouts. The overall gel diameters that can be achieved depend on the spinneret dimensions, the extrusion rate at which the gel is passed through it and the speed at which the stage is moved.

Table 2: Overview of spinneret designs, dimensions (OD: outer diameter, ID: inner diameter), examples of resulting conduit structures, parameters for fabrication and spinneret limitations. Extrusion conditions are given in stage speed (mm sec^{-1}) and extrusion rate (ml min^{-1}).

Spinneret	Needle Gauge (OD/ID mm)	Structure Layout	Example of 3D structure	Materials and Extrusion conditions	Possible Layout and Size Spectrum
coaxial	17 (1.47/1.07) 24 (0.57/0.31)			2% Alg_M SS_{50} 11.9/0.5	1 filament, centered 100 µm – 2 mm
4-lumen	14 (2.11/1.60) 27 (0.41/0.21)			2% Alg_M 2 PLA_{115} 2 SS_{50} 4.8/0.8	1 - 4 filaments, off centre 1 – 3 mm
5-lumen	12 (2.77/2.16) 27 (0.41/0.21)			2% Alg_M 5 Fe_{65} 4.8/1.2	1 – 5 filaments, off centre 1.5 – 4 mm
5x-lumen	13 (2.4/1.8) 27 (0.41/0.21)			1% Alg_L 4 SS_{50} 4.8/0.8 Gellan Gum Microgel with PC12 cells 4.8/0.05	up to 2 gels 1 filament, centered 1 – 4 filaments, off centre 1.5 – 3.5 mm
triaxial	17 (1.5/1.1) 21 (0.82/0.51) 28 (0.36/0.18)			2% Alg_L 4.8/0.4 0.5% GG + PC12s 4.8/0.05 SS_{50}	up to 2 gels 1 filament, centered 200 µm – 2 mm

The incorporation of different materials in a controlled fashion was of particular interest when developing the system for the fabrication of improved artificial conduits. As a result of this, spinnerets with up to three different inlet ports have been custom built, allowing the incorporation of fibres and two different gel or liquid compositions. Using this approach, cells can be placed into a separate part of the structure, which allows the creation of a better suited environment using softer and more porous gels, while the other part of the structure, made of a stronger gel, holds the filaments and maintains structural integrity.

Filaments made of different materials with a variety of sizes and surface finishes have been incorporated into coaxial gel fibres to investigate the versatility as well as limitations of the system with regards to the filaments that can be encapsulated. Figure 6 shows a selection of filaments, which were successfully embedded into alginate. The lumen diameter of the inner needle of the coaxial spinneret has a size of 310 μm, allowing filaments of a maximum cross-sectional width of 300 μm to be fed through. Single or multiple filaments in a size range of 50 – 150 μm, of hydrophobic or hydrophilic materials with smooth and rough surfaces were embedded into homogenous gel layers. This included SS_{50} (Figure 6A&B), SS_{150}, PLA_{150} (Figure 6C&D), rGO-PPy (Figure 6E&F) and multi-filament CFT (Figure 6G&H). The encapsulation of 280 μm Nylon was not successful. During the extrusion process a continuous fibrous gel of alginate was formed, however it was not attached to the filament, and did not sufficiently encapsulate it. As encapsulation of other hydrophobic filaments was achieved, the large diameter in relation to the needle size or a combination of the large diameter and the hydrophobic behaviour of the filament are most likely to have prevented the encapsulation within gel. This could be addressed by applying a surface treatment to the filaments to increase their hydrophilicity or by roughening the surface. Overall a broad range of filaments was successfully encapsulated into alginate, including rough, weak filaments (rGO-PPy); smooth, elastic filaments (PLA_{115}) and bundles of very fine filaments (CFT), which, depending on the filament, introduce properties such as electroactivity, conductivity and the potential for controlled drug release into the 3D hydrogel construct.
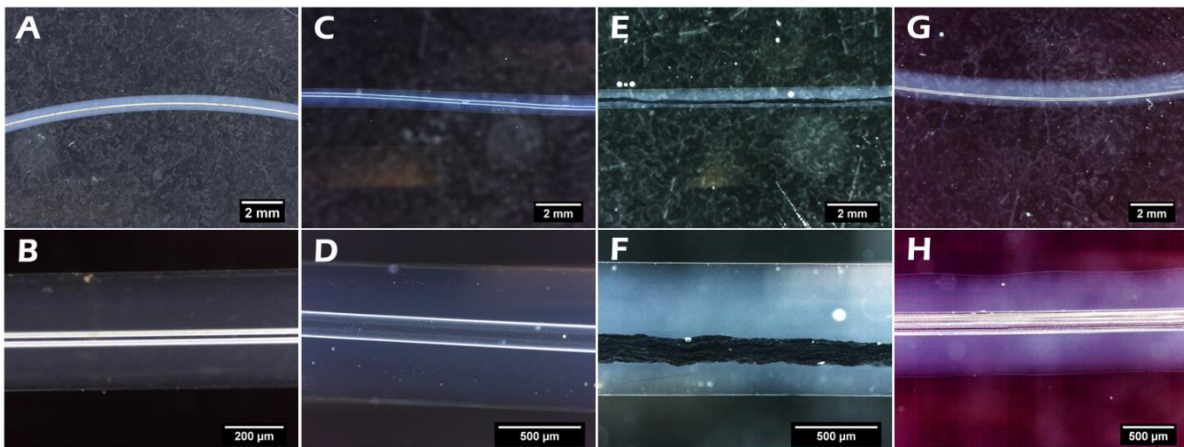
Figure 6: Filaments of different size, materials and surface structure that have been encapsulated into alginate gel. A&B: SS_{50}, 11.9 mm sec^{-1}/0.5 ml min^{-1}; C&D: PLA_{150}, 4.8 mm sec^{-1}/0.5 ml min-1; E&F: rGO-PPy, 4.8 mm sec^{-1}/0.5 ml min^{-1}, G&H: CFT, 4.8 mm sec^{-1}/0.5 ml min^{-1}.

The method also allows for a range of filament shapes to be incorporated. Not only filaments with a circular cross section and homogenous axial diameter can be encapsulated into gel, but

also filaments with an irregular axial diameter as well as fibres with cross sections different from circular shape. To demonstrate this capability, three SS_{50} filaments were manually braided before being fed through the coaxial spinneret. 1% Alg_M was extruded around the braided filaments at an extrusion rate of 0.5 ml min^{-1} and stage speed set to 4.8 mm sec^{-1} (Figure 7A-B). Incorporation of a hydrophobic filament will lead to the formation of a hollow lumen around the filament, resulting from a lack of interaction between the hydrogel and the filament. As shown in Figure 7C-D a hydrophobic star-shaped PLA filament was embedded into the hydrogel creating a lumen around the filament. The same result was observed for PLA filaments with a circular cross section. In contrast no hollow lumen was observed when hydrophobic CFT or rGO-PPy were encapsulated, which is most likely a result of the rough and uneven surface topography of these filaments.

To further increase the versatility and areas of application of the extruded structures, filaments were encapsulated into alginate and removed following the extrusion process, leaving empty or backfilled channels of controlled size and shape (Figure 7E-H). To backfill the gel channels the encapsulated filament was removed while the structure was submerged into a dispersion of spherical 50 nm sized polypyrrole particles (Figure 7G), or a suspension of PC12 cells in cell culture media (Figure 7H).

The diameter of the channels is dictated by the size of the filament encapsulated. Removal of filaments is uncomplicated as long as the matrix material does not adhere to the surface of the filament, which makes SS or PLA good materials for removal from hydrogels. SS filaments with a diameter of 50 – 150 µm were easily removed from extruded alginate fibres. Channels formed by 50 µm filaments show smooth and evenly spaced walls, with the diameter within 2µm of the filament diameter. When removing the 150 µm filament the resulting channel had rougher walls, which were up to 25 µm larger than the filament. As a result of their thickness, the 150 µm filaments are stiffer compared to the 50 µm filaments. In the case of the 150 µm SS filaments the structure of the gel was dictated by the shape of the filaments as opposed to the shape of a gel, i.e. a filament that is not absolutely straight, but instead slightly curved as a result of being stored on a spool, will cause the gel to follow the same curve as the filament if the filament is stronger than the extruded hydrogel. That is the case when the SS_{150} filaments are embedded in the hydrogel. When removing these filaments from the gel the channels become distorted as the filament does not bend with the gel during removal. This also causes the rougher surface on the inside of the channels, as the relatively sharp end of the filament scratches along the walls, leaving them with a rough texture.

18

When backfilling the channels while removing the SS_{150} filament, these effects were observed to be less pronounced. This could be a result of the added lubrication from the liquid that is drawn into the channel. Channels produced using SS_{150} filaments were uncomplicated to backfill with aqueous based solutions containing nanoparticles (50 nm) or PC12 cells (10 – 20 µm).
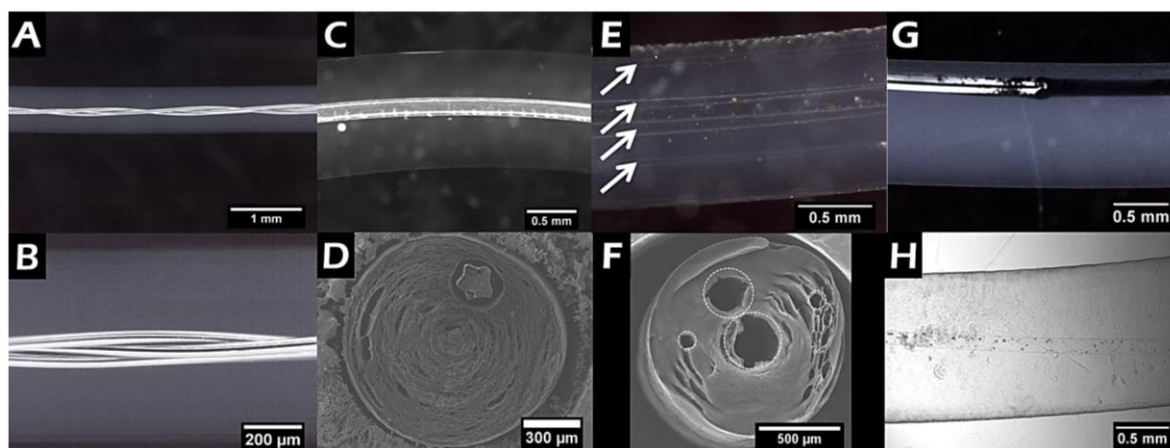

Figure 7: Structural versatility of extruded hydrogels containing filaments. A&B: 3 manually braided SS_{50} filaments embedded into 2% Alg_M (4.8 mm sec^{-1}/0.4 ml min^{-1}). C&D: PLA_+ filament embedded into 2% Alg_M (4.8 mm sec^{-1}/0.5 ml min^{-1}). E&F: 2 SS_{50} and 2 SS_{150} encapsulated into 2% Alg_L and removed after extrusion. White arrows indicate the 4 resulting channels. G&H: Backfilling of 2% Alg_L extruded gels by removing the SS_{150} filament as the structure was submerged into either a dispersion of spherical 50 nm sized polypyrrole particles (G) or a suspension of PC12 cells in cell culture media (H).

The ability to backfill size-controlled channels within the fibrous 3D hydrogel structure opens up a different level of versatility. On one hand this method has the benefit of creating very homogenously sized channels, as well as much smaller channels than those that can usually be achieved in traditional coaxial wet-spinning approaches. These utilise lower concentration of coagulant or plain water to inject into the spinning process creating coagulant or water filled channels within the gel. Additionally this new technique creates the possibility of backfilling the channels with materials or cells that cannot be incorporated into the wet-spinning process due to incompatibility with the coagulant or the un-crosslinked spinning solution. Furthermore, it allows more versatile use of one spinneret configuration as no sealed syringe attachment ports are required to inject the solution during the spinning process.

1.4.3 Cell Compatibility of Filament Encapsulation

PC12 cells were encapsulated into alginate gel which had been extruded around four SS_{50} filaments. The viability of the cells was analysed at three time points after the extrusion by selectively staining live and dead cells. As can be seen from the graph in Figure 8A, the viability of the cells was above 90% for all time points. The low percentage of dead cells at 3 h ($4.9 \pm 1.6\%$) after the extrusion indicates that the extrusion process itself is cell

compatible and does not induce cell death due to unfavourable conditions. After culturing the cell-filled construct for 4 days, the viability was still observed to be in a normal range ($94.2 \pm 2.5\%$), indicating that the cells are sufficiently supplied with nutrients over the period tested. As can be observed from the average live cell numbers at each time point, proliferation of the cells is limited. A significant increase in cell number was observed after 24 h compared to 3h with no further increase after 4 days of culturing post fabrication. This is a phenomenon that has previously been observed with cells encapsulated in alginate [32]. The lack of cell binding motifs and the dense encapsulation lead to inert cell behaviour where cells are viable and metabolically active, without showing great adhesion, proliferation or differentiation. The lack of attachment to encapsulating gels can be mitigated by chemically modifying the alginate gel with cell adhesion-promoting peptides, utilizing a different material composition or encapsulating the cells in a different part of the structure using a softer, more porous hydrogel.
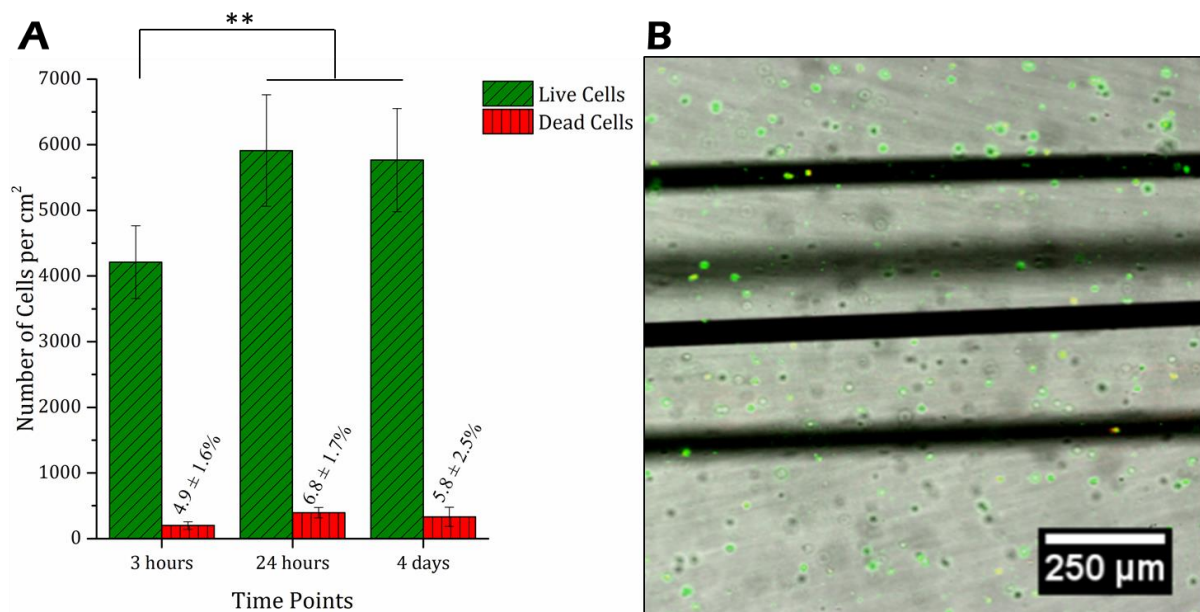
Figure 8: Alginate encapsulating PC12 cells and four 50 μm stainless steel wires. A: Number of live (green, diagonal lines) and dead (red, vertical lines) cells per cm^2, with the percentage of dead cells and significant differences in cell number. B: alginate encapsulating cells (round dots) and filaments (black lines).

1.5 Conclusion

Here we have presented a reliable semi-automated method to create a variety of 3D fibrous structures that are based on filaments encapsulated within hydrogels. A wide range of filaments (size, shape, material) can be embedded controllably into positions throughout the hydrogel. The positioning, number of filament elements and overall size of the structure are mostly dependent on the spinneret design, however diameters can be varied greatly by

adjusting the extrusion rate of the gel as well as the speed at which the stage translates, allowing high controllability while offering versatility within one setup. Further potential applications are opened up by removing filaments from the gel, creating precisely sized channels which can be left empty or backfilled with other solutions including those containing living cells or particles. When used with alginate and a calcium bath as the coagulant, this method shows great cytocompatibility with cells extruded straight into the structure.

The method introduced here can address the difficulties of combining all desired properties for the "ideal" nerve conduit together in one structure (Figure 9). The overall size of the extruded gel is within the range required for use as a conduit and can be varied on demand. The porosity of the structure can be tailored by choosing the right material configuration and supported by the incorporation of hollow channels within the gel, controlled drug release can be achieved by incorporating drug laden fibres or spheres, electrical conductivity and electroactivity can be introduced using fibres from organic conducing materials or other inherently conducting materials. Physical guidance for regrowing nerve fibres can be provided by small encapsulated filaments or channels that are created by the removal of filaments. The incorporation of living cells can either be achieved by introducing the cells into the gel during the extrusion process, or backfilling them into channels by removing the filaments.
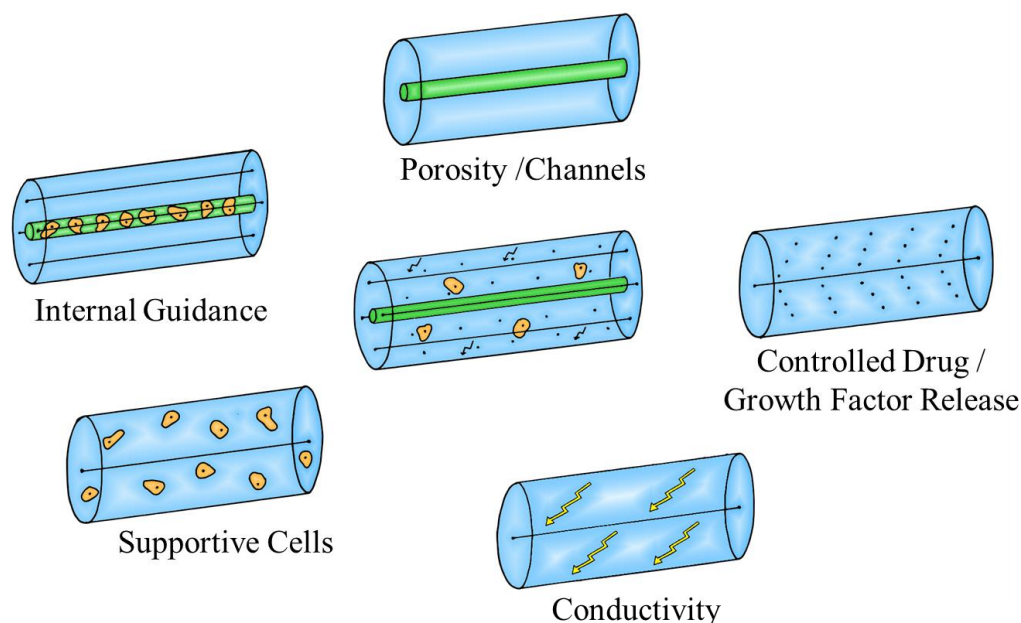
Figure 9: Schematic of nerve conduit deigns achieved through use of the developed technique.

Overall, if a lower level of controllability is sufficient for the desired application, this setup can be simplified and built up in an inexpensive manner using less sophisticated hardware with respect to the stage and syringe pump. Miniaturization of the system is again possible if a more portable build is desired. Furthermore we envision that this technique can be of use to other fields outside of peripheral nerve regeneration where fibrous hydrogels with controlled features and properties are required, including actuation in the field or artificial muscles, general microfluidics applications and the broader field of regenerative tissue engineering.

1.6 Acknowledgements

1.7 References

1. Khan, F., M. Tanaka, and S.R. Ahmad, *Fabrication of polymeric biomaterials: a strategy for tissue engineering and medical devices.* Journal of Materials Chemistry B, 2015.
2. Kramschuster, A. and L.-S. Turng, *17 - Fabrication of Tissue Engineering Scaffolds*, in *Handbook of Biopolymers and Biodegradable Plastics*. 2013, William Andrew Publishing: Boston. p. 427-446.
3. Hart, A., G. Terenghi, and M. Wiberg, *Tissue Engineering for Peripheral Nerve Regeneration*, in *Tissue Engineering*, N. Pallua and C.V. Suscheck, Editors. 2011, Springer Berlin Heidelberg. p. 245-262.

4.   Jiang, X., et al., *Current applications and future perspectives of artificial nerve conduits.* Experimental Neurology, 2010. **223**(1): p. 86-101.

5.   Arslantunali, D., et al., *Peripheral nerve conduits: technology update.* Med Devices (Auckl), 2014. **7**: p. 405-24.

6.   de Ruiter, G.C.W., et al., *Designing ideal conduits for peripheral nerve repair.* Neurosurgical Focus, 2009. **26**(2): p. E5.

7.   Gu, X., et al., *Construction of tissue engineered nerve grafts and their application in peripheral nerve regeneration.* Progress in Neurobiology, 2011. **93**: p. 204-230.

8.   Daly, W., et al., *A biomaterials approach to peripheral nerve regeneration: bridging the peripheral nerve gap and enhancing functional recovery.* Journal of The Royal Society Interface, 2011. **9**(67): p. 202-221.

9.   Gordon, T., O.A.R. Sulaiman, and A. Ladak, *Electrical Stimulation for Improving Nerve Regeneration: Where Do We Stand?* Essays on Peripheral Nerve Repair and Regeneration, 2009. **87**: p. 433-444.

10.   Deumens, R., et al., *Repairing injured peripheral nerves: Bridging the gap.* Progress in Neurobiology, 2010. **92**(3): p. 245-276.

11.   Dinis, T.M., et al., *3D multi-channel bi-functionalized silk electrospun conduits for peripheral nerve regeneration.* Journal of the Mechanical Behavior of Biomedical Materials, 2015. **41**: p. 43-55.

12.   Abidian, M.R., et al., *Hybrid Conducting Polymer-Hydrogel Conduits for Axonal Growth and Neural Tissue Engineering.* Advanced Healthcare Materials, 2012. **1**(6): p. 762-767.

13.   Lee, T.H., et al., *Functional Regeneration of a Severed Peripheral Nerve With a 7-mm Gap in Rats Through the Use of An Implantable Electrical Stimulator and a Conduit Electrode With Collagen Coating.* Neuromodulation, 2010. **13**(4): p. 299-305.

14.   Quigley, A.F., et al., *Engineering a multimodal nerve conduit for repair of injured peripheral nerve.* Journal of neural engineering, 2013. **10**(1): p. 016008.

15.   Wu, H., et al., *Mechanical properties and permeability of porous chitosan-poly(p-dioxanone)/silk fibroin conduits used for peripheral nerve repair.* J Mech Behav Biomed Mater, 2015. **50**: p. 192-205.

16.   Pabari, A., et al., *Recent advances in artificial nerve conduit design: Strategies for the delivery of luminal fillers.* Journal of Controlled Release, 2011. **156**(1): p. 2-10.

17.   Luo, H.Y., et al., *Fabrication of viable centimeter-sized 3D tissue constructs with microchannel conduits for improved tissue properties through assembly of cell-laden microbeads.* Journal of Tissue Engineering and Regenerative Medicine, 2014. **8**(6): p. 493-504.

18.   Yudin, V.E., et al., *Wet spinning of fibers made of chitosan and chitin nanofibrils.* Carbohydr Polym, 2014. **108**: p. 176-82.

19.   Nelson, K.D., et al., *Technique paper for wet-spinning poly(L-lactic acid) and poly(DL-lactide-co-glycolide) monofilament fibers.* Tissue Eng, 2003. **9**(6): p. 1323-30.

20.   Yang, C.Y., et al., *Fabrication of porous gelatin microfibers using an aqueous wet spinning process.* Artif Cells Blood Substit Immobil Biotechnol, 2009. **37**(4): p. 173-6.

21.   Hu, M., et al., *Hydrodynamic spinning of hydrogel fibers.* Biomaterials, 2010. **31**(5): p. 863-9.

22.   Hardy, J.G., L.M. Romer, and T.R. Scheibel, *Polymeric materials based on silk proteins.* Polymer, 2008. **49**(20): p. 4309-4327.

23. Onoe, H., et al., *Metre-long cell-laden microfibres exhibit tissue morphologies and functions.* Nature Materials, 2013. **12**(6): p. 584-590.

24. Cornock, R., et al. *Precision wet-spinning of cell-impregnated alginate fibres for tissue engineering.* 2013. Fiber Society.

25. Chikar, J.A., et al., *The use of a dual PEDOT and RGD-functionalized alginate hydrogel coating to provide sustained drug delivery and improved cochlear implant function.* Biomaterials, 2012. **33**(7): p. 1982-90.

26. Pfister, L.A., et al., *Controlled nerve growth factor release from multi-ply alginate/chitosan-based nerve conduits.* Eur J Pharm Biopharm, 2008. **69**(2): p. 563-72.

27. Chan, L.W., X. Liu, and P.W. Heng, *Liquid phase coating to produce controlled-release alginate microspheres.* J Microencapsul, 2005. **22**(8): p. 891-900.

28. Basavaraja, C., et al., *Electrical conduction mechanism of polypyrrole-alginate polymer films.* Macromolecular Research, 2010. **18**(11): p. 1037-1044.

29. Sajesh, K.M., et al., *Biocompatible conducting chitosan/polypyrrole-alginate composite scaffold for bone tissue engineering.* International Journal of Biological Macromolecules, 2013. **62**: p. 465-471.

30. Schirmer, K., et al., *Conductive Composite Fibres from Reduced Graphene Oxide and Polypyrrole Nanoparticles.* Journal of Materials Chemistry B, 2016.

31. Ferris, C.J., et al., *Bio-ink for on-demand printing of living cells.* Biomaterials Science, 2013. **1**(2): p. 224-230.

32. Lee, B.R., et al., *Microfluidic wet spinning of chitosan-alginate microfibers and encapsulation of HepG2 cells in fibers.* Biomicrofluidics, 2011. **5**(2): p. 22208.